Underwater Image Enhancement before Three-Dimensional (3D) Reconstruction and Orthoimage Production Steps: Is It Worth?

Panagiotis Agrafiotis [a,b], Georgios I. Drakonakis [a], Dimitrios Skarlatos [b] and Andreas Georgopoulos [a]

[a] National Technical University of Athens, School of Rural and Surveying Engineering, Lab. of Photogrammetry, Zografou Campus, 9 Heroon Polytechniou str., 15780, Zografou, Athens, Greece; pagraf@central.ntua.gr, georgios.i.drakonakis@gmail.com, drag@central.ntua.gr

[b] Cyprus University of Technology, Civil Engineering and Geomatics Dept., Lab of Photogrammetric Vision, 2-8 Saripolou str., 3036, Limassol, Cyprus; dimitrios.skarlatos@cut.ac.cy

Abstract: The advancement of contemporary digital techniques has greatly facilitated the implementation of digital cameras in many scientific applications, including the documentation of Cultural Heritage. Digital imaging has also gone underwater, as many cultural heritage assets lie in the bottom of water bodies. Consequently, a lot of imaging problems have arisen from this very fact. Some of them are purely geometrical, but most of them concern the quality of the imagery, especially in deep waters. In this paper, the problem of enhancing the radiometric quality of underwater images is addressed, especially for cases where this imagery is going to be used for automated photogrammetric and computer vision algorithms later. In detail, it is investigated whether it is worth correcting the radiometry of the imagery before the implementation of the various automations or not, the alternative being to radiometrically correct the final orthoimage. Two different test sites were used to capture imagery ensuring different environmental conditions, depth, and complexity. The algorithms investigated to correct the radiometry are a very simple automated method, using Adobe Photoshop®, a specially developed colour correction algorithm using the CLAHE (Zuiderveld, 1994) method, and an implementation of the algorithm, as described in Bianco et al. (2015). The corrected imagery is afterwards used to produce point clouds, which in turn are compared and evaluated.

Keywords: underwater 3D reconstruction; underwater image enhancement; SfM-MVS (Structure from Motion-Multi View Stereo)

1. Introduction

A great percentage of mankind's Cultural Heritage lies underwater. Ancient ports, seaside fortifications, and shipwrecks are only but a few examples of underwater Cultural Heritage. These assets wait to be documented according to article 16 of the Venice Charter (ICOMOS 1964). However, the underwater environment is very hostile for humans and for digital equipment alike. Nowadays, technological advances have enabled the use of automated algorithms for mapping and three-dimensional (3D) modelling using digital imagery, while the highly sensitive equipment needs special protection. In addition, digital RGB imagery is adversely affected by the underwater conditions, and its radiometry is rapidly deteriorating with depth. Because, nowadays, most of the documentation procedures are based on digital image processing (Drap 2012; Henderson et al., 2013; Johnson-Roberson et al., 2016), a thorough investigation into the resulting radiometry of the original images and the final imagery products seems necessary.

Within this context, this paper investigates the effect of several algorithms that correct the underwater imagery radiometry and assesses their suitable implementation moment, i.e. before or after processing and the production of the finale orthoimage. As illumination and colour loss is rapid underwater and this largely depends on depth, this research focuses on the investigation of the behaviour of the RGB channels and the algorithms that are available to restore their natural values.

For this purpose, two different approaches for underwater image processing are implemented according to their description in literature. The first one is image restoration. It is a strict method that is attempting to restore true colours and correct the image using suitable models, which parameterize adverse effects, such as contrast degradation and backscattering, using image formation process and environmental factors, with respect to depth (Hou et al., 2007, Treibitz and Schechner, 2009). The second one uses image enhancement techniques that are based on qualitative criteria, such as contrast and histogram matching (Ghani and Isa, 2014, Iqbal et al., 2007 and Hitam et al., 2013). Image enhancement techniques do not consider the image formation process and do not require environmental factors to be known a priori (Agrafiotis et. al., 2017).

Visual computing in underwater settings is particularly affected by the optical properties of the surrounding medium (von Lukas 2016). The goal of the presented work is to investigate the effect of the underwater imagery preprocessing on the 3D reconstruction of the scene using automated Stuctrure from Motion (SfM) and Multi View Stereo (MVS) software. An additional aim is to present measurable results regarding the effect of this preproccessing on the produced orthoimages. Since the processing of images, either separately or in batch, is a time-consuming procedure that has high compotutational cost requirements, it is critical to determine the necessity of implementing colour correction and enhancement

before the SfM - MVS procedure or directly to the final orthoimage when this is the deliverable.

2. Materials and Methods

In order to address the above research issues, two different test sites were selected to capture underwater imagery ensuring different environmental conditions (i.e. turbidity, waves etc.), depth, and complexity. In addition, three different image correction methods are applied to these datasets: A very simple automated method using Adobe Photoshop, a colour correction algorithm, which was developed using the CLAHE (Zuiderveld, 1994) method, and an implementation of the algorithm described in Bianco et al. (2015). Subsequently, dense 3D point clouds (3Dpc), 3D meshes, and orthoimages were generated for each dataset using a commercial SfM - MVS software. The produced 3D point clouds were then compared using Cloud Compare (CloudCompare 2.8.1, 2016) open-source software, while the resulting orthoimages were compared using both their visual appearance and their histograms.

2.1. Test Datasets

2.1.1. Shallow Waters

The dataset created for shallow waters (Figure 1a) is a near-shore underwater site situated at depths varying from 2 to 3 meters, and presents smooth depth changes (Figure 2a). Image acquisition took place with a Nikon DSLR D5200, with 24 MP sensor and pixel size of 3.92 μm and by using an 18-55 mm lens set at 18 mm, and an Ikelite dome housing. No artificial light sources were used due to the small depth. Because of the wind, the wavy surface of the water creates dynamic sun flicker (caustics) on the seabed. Waves also resulted into water turbidity, and thus very poor visibility conditions. The camera positions of this dataset follow a typical phtogrammetric distribution (Figure 3a), with obvious parallel dive paths.

2.1.2. Deep Waters

The amphorae dataset is an artificial reef constructed using 1m long amphorae, replicas from Mazotos shipwreck (Demesticha, 2010) and presents abrupt changes on the imaged object depth (Figure 2c). They are positioned on the sea bottom at 23 meters depth, stacked together in two layers, with 25 and 16 amphorae, respectively (Figure 1b). Their placement is assumed to be similar to their original position in the cargo area of the ship. Photography took place with an action camera, Garmin Virb XE camera, with 12MP sensor with 1.5μm physical pixel size. Four LED video lights of 300LX eatc, were mounted next to the camera, to enhance the recorded colour information. In contrast with the shallow waters

dataset, camera positions do not follow a specific pattern (Figure 3b). As it is expected, due to its depth for the shallow waters dataset, green and blue are the dominant colours, while a percentage of red colour is also present (Figure 4a). In contrast, in the deep waters dataset, blue is the dominant colour, while green follows. Although red channel absorption is strong in such depths, red is still present in the histogram (Figure 5b) of the images, depending on the artificial lighting and on the camera to object distance.

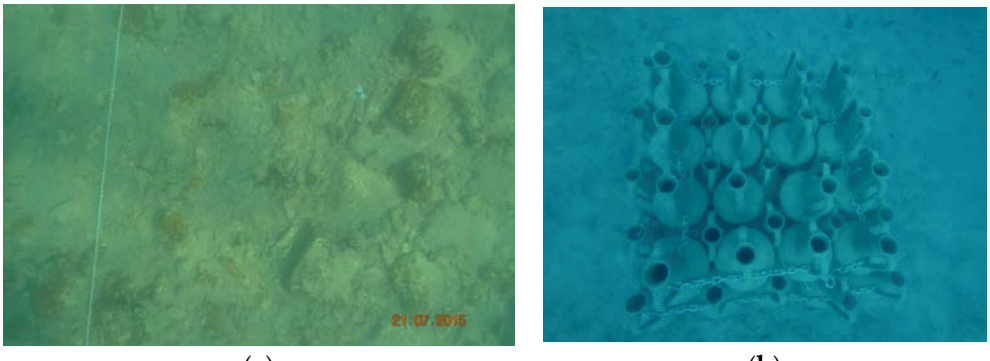

(**a**) (**b**)

Figure 1. Sample images from shallow waters dataset (**a**) and deep waters dataset (**b**).

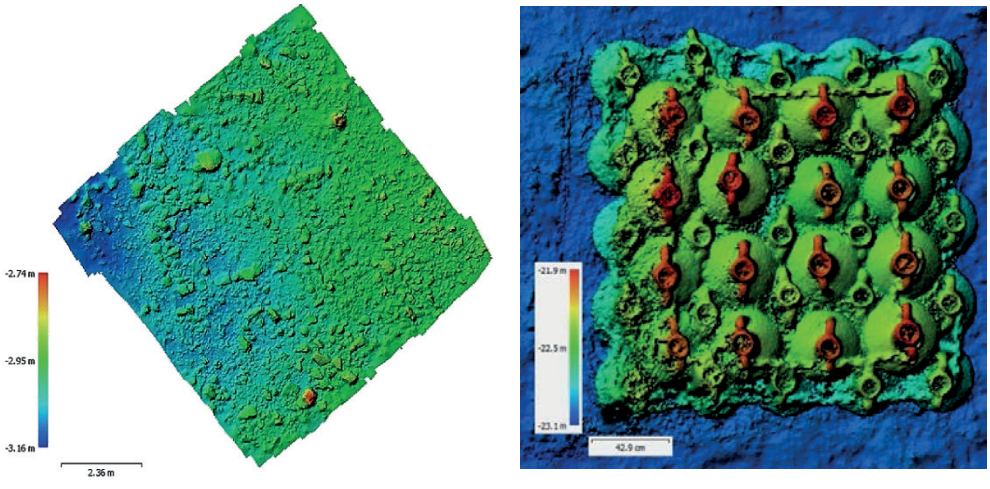

(**a**) (**b**)

Figure 2. Resulted Digital Surface Model (DSM) for shallow waters dataset (**a**) and deep waters dataset (**b**). The difference in depth range between the two datasets is profound.

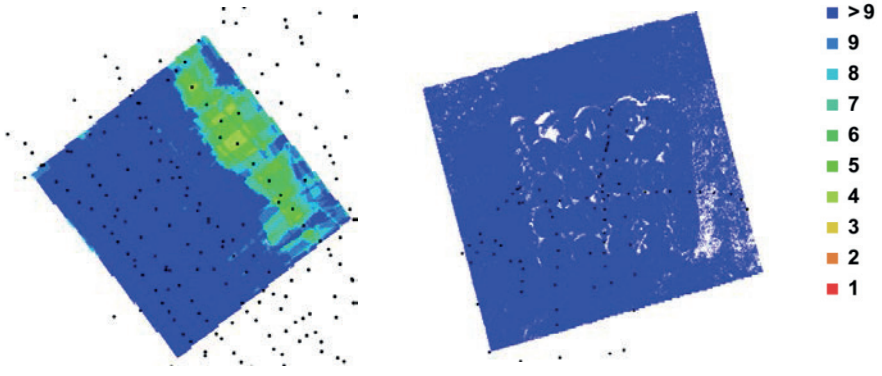

(**a**) (**b**) (**c**)

Figure 3. Camera positions and number of overlapping images used for shallow waters dataset (**a**) and deep waters dataset (**b**). In (**c**) the image overlap colour scale.

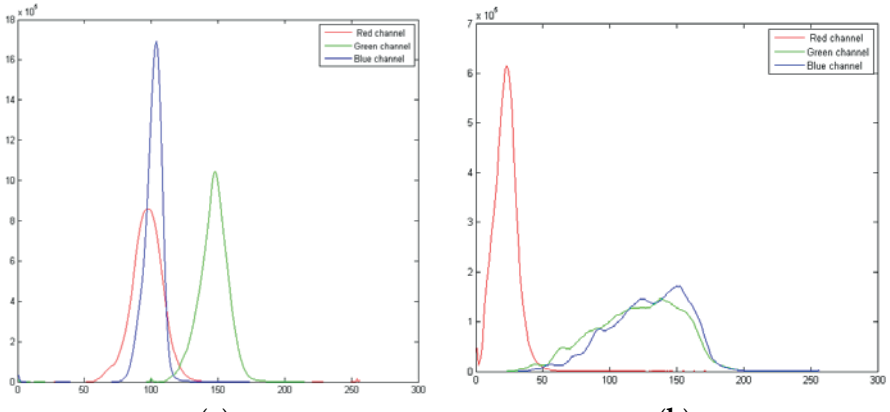

(**a**) (**b**)

Figure 4. The respective histograms of the sample images from shallow waters dataset (**a**) and deep waters dataset (**b**).

2.2. The Applied Image Correction Algorithms

2.2.1. Clahe Based Algorithm

Adaptive histogram equalization (AHE) is a computer image processing technique that is used to improve contrast in images. Contrast Limited AHE (CLAHE) differs from ordinary adaptive histogram equalization in its contrast limiting. The CLAHE (Zuiderveld, 1994) algorithm partitions the image into contextual regions and applies the histogram equalization to each one, while it limits the contrast. This evens out the distribution of used grey values, and thus makes hidden features of the image more visible. The CLAHE algorithm has been

used extensively in underwater image correction in the literature (Kumar Rai, et al. 2012; Yussof, et al., 2013; Singh, et al., 2011 and Hitam et al., 2013). Recently, CLAHE was used for the dehazing of underwater video for an augmented reality application (Bruno et al., 2017) presenting interesting results in real time scenarios.

The implemented image enhancement algorithm separates image channels of RGB colour space. Then a histogram equalization process is applied to each channel. A Rayleigh Cumulative Distribution Function (CDF) was created for the equalization. The CDF range is from 0 to 255, in order to match the pixel intensity values and its maximum value was appointed to one-third of the total range (76.5). Afterwards, the CLAHE (Zuiderveld, 1994) algorithm was applied to each channel. Partition size and contrast clipping were determined experimentally. Rayleigh distribution was used again as the transformation function parameter. Finally, the algorithm composes all three channels and the output is the colour corrected image.

In the shallow waters dataset, applying histogram equalization using a Rayleigh CDF on each colour channel results in histograms of practically identical shape. This dramatically improves image sharpness and its colours seem to be restored. In the deep waters dataset the algorithm was modified in order to cope with the large depth conditions. The red channel was not equalized before CLAHE algorithm correction, while green and blue channels were equalized with a different CDF in order to restrict their intensity into lower values.

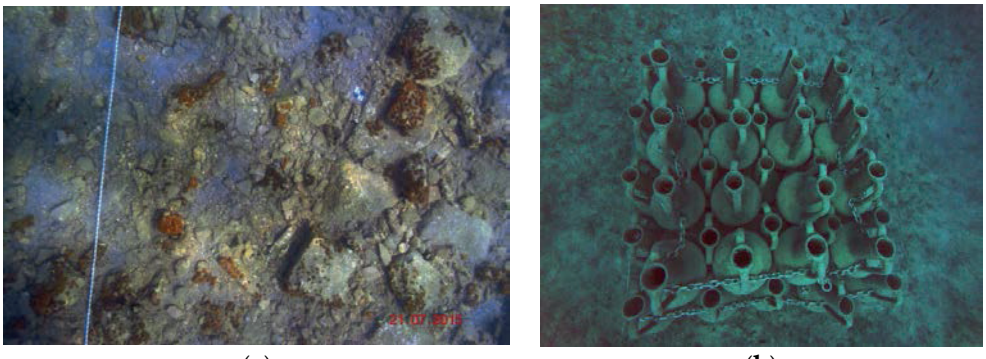

(**a**) (**b**)

Figure 5. Corrected imagery with Contrast Limited adaptive histogram equalization (CLAHE) based algorithm for shallow (**a**) and deep (**b**) water.

2.2.2. Algorithm of Bianco et al. (2015)

The imagery was also processed using the algorithm presented by Bianco et al., (2015), where colour correction of underwater images is performed by using lab colour space. In more detail, the chromatic components are changed moving their distributions around the white point (white balancing), and histogram cut-off and stretching of the luminance component is performed to improve the image

contrast. Main constrains of this method are the grey-world assumption and the uniform illumination of the scene (Bianco et al., 2015).

In the shallow water dataset, the corrected imagery looks very realistic as all of the colours are correctly enhanced. However, the sharpness of the imagery is not well improved. In the deep waters dataset, the corrected image presents an enhanced contrast despite the fact that the image looks similar to greyscale due to the absence of the red colour at such depths.

(**a**) (**b**)

Figure 6. Corrected imagery with Lab for shallow (**a**) and deep (**b**) water.

2.2.3. Adobe Photoshop® (Adobe Photoshop CS5, (2010))

Additionally, images were processed with Adobe Photoshop in order to enhance the contrast and sharpness. Automated algorithm "*Find Dark and Light Colours*" was used for this correction. According to the software, this algorithm analyzes the image in order to find dark and light colours, and uses them as the shadow and highlight colours. The option "*Snap Neutral Midtones*" was also checked. This adjusts the midtones so that colours that are close to neutral are mapped to the target neutral colour.

In the shallow waters dataset, image blurriness is reduced and colours become more realistic. In contrast, the correction has little effect on the imagery that is acquired in deep waters. Contrast is slightly increased, while colours remain unaffected. For the deep waters dataset, this method was proven ineffective and a different algorithm was used. It clips colour channels identically in order to increase contrast while it preserves the original colours. The final image is improved partially. Red prevails on the image corners because of the chromatic aberration effect provoked by the fish-eye lens of the action camera.

To sum up, for the shallow waters dataset, all of the correction algorithms improve the colours of the imagery. The CLAHE based algorithm improves more the image sharpness, however, the more realistic colours are obtained by using the algorithm of Bianco et al., (2015). For the deep waters dataset, the results of Adobe Photoshop and CLAHE based algorithms present more percentage of red values,

and thus the imagery looks more appealing to the human eye. However, again, the results of the algorithm of Bianco et al., (2015) resemble more to the underwater environment reality, even if the red colours are undervalued. Important to note is the overincreased red values on the pixels of the corners of the deep water dataset (Figure 7b). This phenomenon is usually observed when robust colour correction methods are applied in imagery that is produced by action cameras using fish-eye lenses.

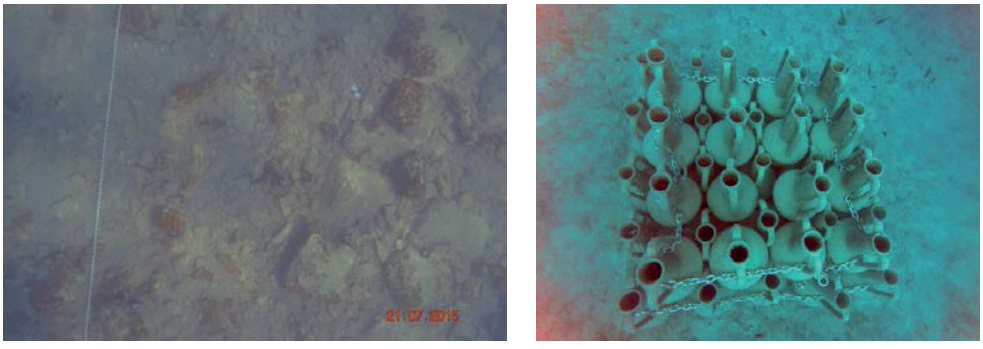

(**a**) (**b**)

Figure 7. Corrected imagery with Adobe Photoshop® for shallow (**a**) and deep (**b**) waters.

2.3. SfM-MVS Processing

These image enhancement methods were evaluated by visual inspection and histogram comparison. Subsequently, corrected image were processed using SfM-MVS with Agisoft's Photoscan commercial software (AgiSoft PhotoScan Professional 1.2.6, 2016).). To this end, four different three-dimensional (3D) projects were created for each test site: (i) One with the original uncorrected imagery, which is considered the initial solution, (ii) a second one using the developed correction algorithm applying CLAHE (Zuiderveld, 1994), (iii) a third one using the imagery that resulted implementing the colour correction algorithm presented in Bianco et al., (2015), and (iv) a fourth one using Adobe Photoshop enhanced imagery. All three channels of the images were used for these processes.

For the created projects of each test site, the alignment parameters of the original (uncorrected) dataset were used as the corrected images were replacing the uncorrected ones by changing the image path. This ensured that the alignment parameters were the same in order to test only the number of points that were extracted for the dense cloud. In order to scale the 3D dense point clouds, predefined Ground Control Points (GCPs) were used for the shallow water projects. These GCPs were mesured using a Total Station from the shore. Scalebars were used for scaling of the deep water dataset projects since it was impossible to use traditional surveying methods due to the depth. Subsequently, 3D dense point

clouds of medium quality and density were created for each data set. No filtering during this process was performed in order to get the total number of dense point clouds, also the noise. It should be noted that medium quality dense point cloud means that the initial images' resolution was reduced by factor of 4 (2 times by each side), in order to be processed by the SfM-MVS software (Agisoft, 2017).

Table 1 sums up the results of the aforementioned processing for medium quality dense point cloud generation. For the shallow waters dataset, an area of 21.3 m² was covered by 155 images, having an average camera to object distance 1.57 m, and thus resulting to a ground resolution of 0.304 mm/pixel (Figure 8). For the deep water dataset, an area of 8.01 m² was covered by 89 images, having an average camera to object distance 1.68 m, and thus resulting to a ground resolution of 0.743 mm/pixel (Figure 11). It must be noted that the percentages of the differences of dense point cloud number resulting from the processed images in comparison to the dense point cloud resulted from the original ones are not significant. These differences are magnified when it comes to the deep waters dataset and this is probably due to the complexity of the object in respect with image correction methodology.

Table 1. Results of the Stuctrure from Motion (SfM)- Multi View Stereo (MVS) procedure for medium quality dense cloud generation.

Dataset used	Colour Correction Method	Focal Lenght (mm)	Pixel Size (μm)	Average Camera to Object Distance (m)	Ground Resolution (mm/pixel)	Area Covered (m²)	Reprojection Error (pixel)	Point Number in Dense Point Cloud	Differences of Dense Point Cloud Point Numbers from the Original Ones
Shallow	Original	18	3.92	1.57	0.304	21.3	1.22	20.891.576	-
	CLAHE							20.924.857	0.16%
	Bianco et al. (2015)							19.885.863	-4.81%
	Photoshop							20.841.409	-0.24%
Deep	Original	3	1.5	1.68	0.743	8.01 (top projection)	2.04	6.892.271	-
	CLAHE							7.083.982	2.78%
	Bianco et al. (2015)							6.496.123	-5.75%
	Photoshop							7.222.016	4.78%

2.4. Orthoimage Generation

Orthoimages were created for both test sites. The main aim of this procedure is to determine the necessity of implementing colour correction and enhancement before the SfM-MVS procedure or directly to the final orthoimage when the orthoimage is the deliverable. To this end, orthoimages were generated for every different project using the original imagery (Figures 9a and 12a), the imagery that was corrected with Adobe Photoshop (Figures 9b and 12b), the imagery that was corrected by the CLAHE based algorithm (Figures 9c and 12c), and the imagery that was corrected by the algorithm of Bianco et al., (2015) (Figures 9d and 12d). For the two datasets, the orthoimage Ground Sampling Distance (GSD) was selected to be 0.005 m. Colour correction mode was disabled for all of the datasets since the datasets were not characterized by extreme brightness variations

(Agisoft, 2017), and enabling it would lead to false comparisons and misleading results.

Additionally to this process, the two final orthoimages resulted from the projects of the two test sites using the original imagery (Figures 10a and 13a), were processed with the three colour correction methods (Figures 7b–d and 10b–d) and the results were compared and evaluated. These results are illustrated in Section 3.

(**a**) (**b**) (**c**) (**d**)

Figure 8. Medium quality point cloud for shallow waters dataset from the original imagery (**a**), the imagery corrected by the CLAHE based algorithm (**b**), the imagery corrected by the algorithm of Bianco et al., (2015) (**c**) and the imagery corrected with Adobe Photoshop (**d**).

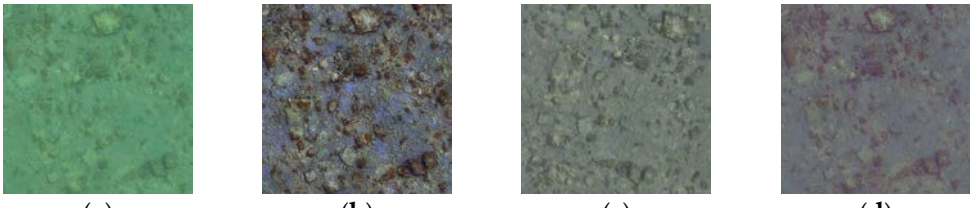

(**a**) (**b**) (**c**) (**d**)

Figure 9. The orthoimage of the shallow dataset created by using the original images (**a**), by using the imagery corrected by the CLAHE based algorithm (**b**), by using the imagery corrected by the algorithm of Bianco et al., (2015) (**c**) and by using the imagery corrected with Adobe Photoshop (**d**) (the dimensions of the imaged area are 4.50 m × 4.50 m).

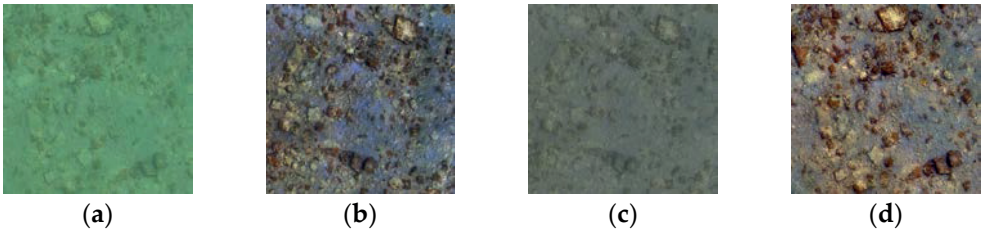

(**a**) (**b**) (**c**) (**d**)

Figure 10. The orthoimage of the shallow dataset created by using the original images (**a**), by correcting the (**a**) using the CLAHE based algorithm (**b**), by correcting the (**a**) using the algorithm of Bianco et al., (**c**), (2015) and by correcting the (**a**) using the Adobe Photoshop (**d**) (the dimensions of the imaged area are 4.50 m × 4.50 m).

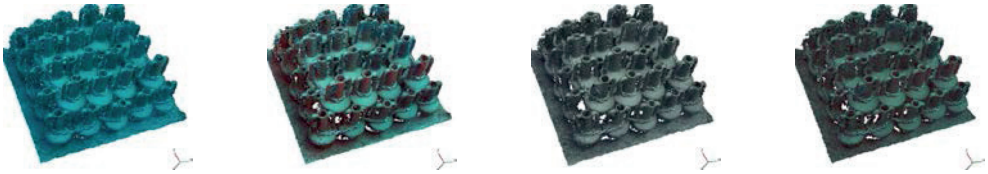

(**a**) (**b**) (**c**) (**d**)

Figure 11. Medium quality point cloud for deep waters dataset from the original imagery (**a**), the imagery corrected with Adobe Photoshop (**b**), the imagery corrected by the algorithm of Bianco et al., (2015) (**c**) and the imagery corrected by the CLAHE based algorithm (**d**).

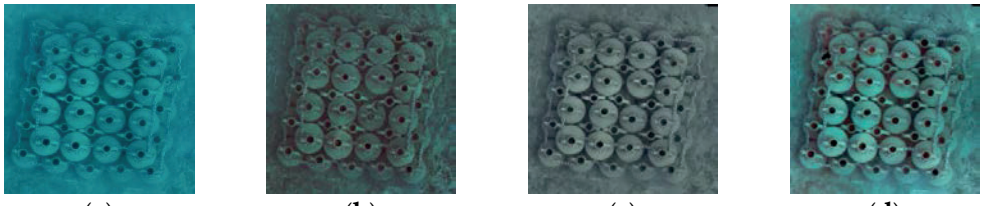

(**a**) (**b**) (**c**) (**d**)

Figure 12. The orthoimage of the deep waters dataset created by using the original images (**a**), by using the imagery corrected by the CLAHE based algorithm (**b**), by using the imagery corrected by the algorithm of Bianco et al., (2015) (**c**), and by using the imagery corrected with Adobe Photoshop (**d**) (the dimensions of the imaged area are 2.30 m × 2.30 m).

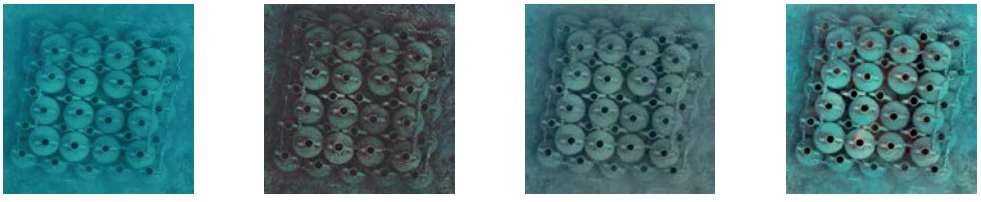

(**a**) (**b**) (**c**) (**d**)

Figure 13. The orthoimage of the deep dataset created by using the original images (**a**), by correcting the (**a**) using the CLAHE based algorithm (**b**), by correcting the (**a**) using the algorithm of Bianco et al., (2015) (**c**) and by correcting the (**a**) using the Adobe Photoshop (**d**)) (the dimensions of the imaged area are 2.30 m × 2.30 m).

3. Evaluation and Results

3.1. Evaluation of the Resulting Orthoimages

When it comes to underwater archaeological projects and excavations, in most of the cases, the main aim of the photogrammetric applications is the generation of accurate and colour consistent 3D model and orthoimages. In this section,

orthoimages using the correcting imagery were generated for each dataset. This was done in order to investigate the necessity of implementing colour correction and enhancement before the SfM-MVS procedure or directly to the final orthoimage, when this is the final deliverable. Two methodologies of orthoimage colour enhancement were used; by applying colour correction on the individual photos of the original data set or directly to the final orthoimage.

By visually inpecting and comparing both the visual appearance and the histograms of the results that are illustrated in Figures 9 and 10 and Figures 12 and 13, one may easily deduce that the implementation of the specific image enhancement techniques does not significantly affect the produced orthoimages. There are only some minor differences between the orthoimages resulting from the corrected imagery and the respective corrected orthoimage.

However, it must be noted that the orthoimages resulting from the corrected imagery of the CLAHE implementation and the Bianco et al., (2015) algorithm are sharper and higher contrasted than the respective directly corrected orthoimages. The opposite happens for the Adobe Photoshop orthoimages for the shallow waters dataset only. These results are confirmed both from tests that were performed by using the shallow waters dataset and the deep waters dataset. This is possibly explained by the fact that when it comes to direct orthoimage colour correction, the necessary computed histograms for colour correction algorithm takes into account a wider variety of colour values at the extent instead of the limited area of a single image.

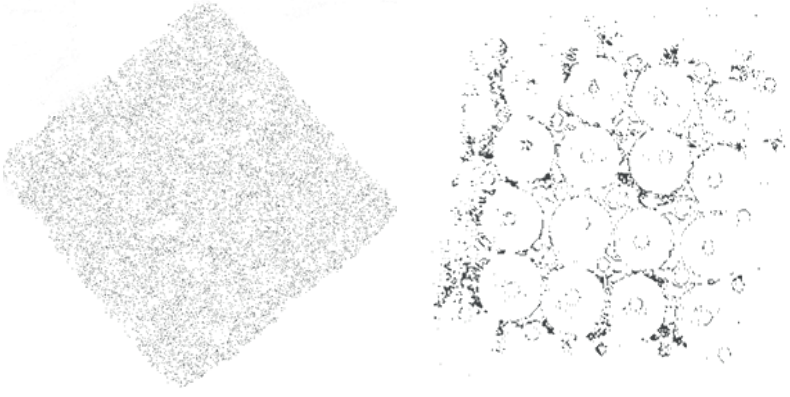

(**a**) (**b**)

Figure 14. (**a**) A result of the subtraction of the shallow waters dataset orthoimages and (**b**) a result of the subtraction of the deep waters dataset orthoimages. Results from all the subtraction are almost the same.

Additionally, orthoimages produced were compared through image subtraction in QGIS software. Orthoimages were inserted to QGIS software and subtracted in respect to the colour correction methods. Results also suggest that

there is not any notable geometric difference between the orthoimages (Figure 14a,b). In more detail, regarding the shallow waters dataset, differences suggest minor geometric defferences that are mainly observed in dark and underexposed areas. The same happens for the deep water dataset. However, in this dataset, changes are more intense due to more dark and underexposed areas existing inbetween the amphorae.

3.2. Test and Evaluation of 3D Point Clouds

The generated dense point clouds were compared within Cloud Compare. Differences between 3D point clouds were illustrated with a colour scale bar (Figure 15a,b and Table 2). In order to ignore outliers, the maximum distance between the respective compared points of each 3D point cloud was set at 0.02m, and the colour scale was divided into eight levels of 0.0025m.

Regarding the tests performed for the shallow waters dataset, in Figures 15a,b and 14c, along with the top view of the result of the comparison, a side view is presented (Figure 15a,b and c bottom) to demonstrate the produced noise in the 3D point cloud. As it is observed in Figures 15a,b and 15c (bottom), these points are the main reason of the existence of points deviating more that 0.003m from the original dense point cloud.

Figures 15d,e,f ,j,k and l present the approximate number of points of the 3D dense point clouds that were created using the corrected images that deviate from the 3D dense point cloud resulting from the original images in relation to the value of that deviation. In Figure 15d,e,f it is observed that over 91% of the points resulted from the corrected images of all the algorithms deviates less than 0.0025 m from the point cloud resulting from the original images. However, all of the points deviated less than 0.005 m. In Figure 15j,k,l it is observed that for the 3D point clouds of the CLAHE corrected imagery, over 34% of the points resulted from the corrected images of all the algorithms deviates less than 0.0025 m from the point cloud resulting from the original images. The respective percentage for Bianco et al., (2015) is 26% and for Adobe Photoshop corrected images 23%. The rest 49% of the 3D point clouds of the CLAHE images represents deviations from 0.0025 m to 0.01 m, while the same percentages for Bianco et al., (2015) is 72.5%, and for Adobe Photoshop corrected images, 69.8%. It is noteworthy that althought the CLAHE has better figurs in under 0.0025 m, the sum of below 0.01m is worse that the other two. The rest 17%, 1.5%, and 7.2% of points, respectively, represent errors from 0.01 to 0.02 m.

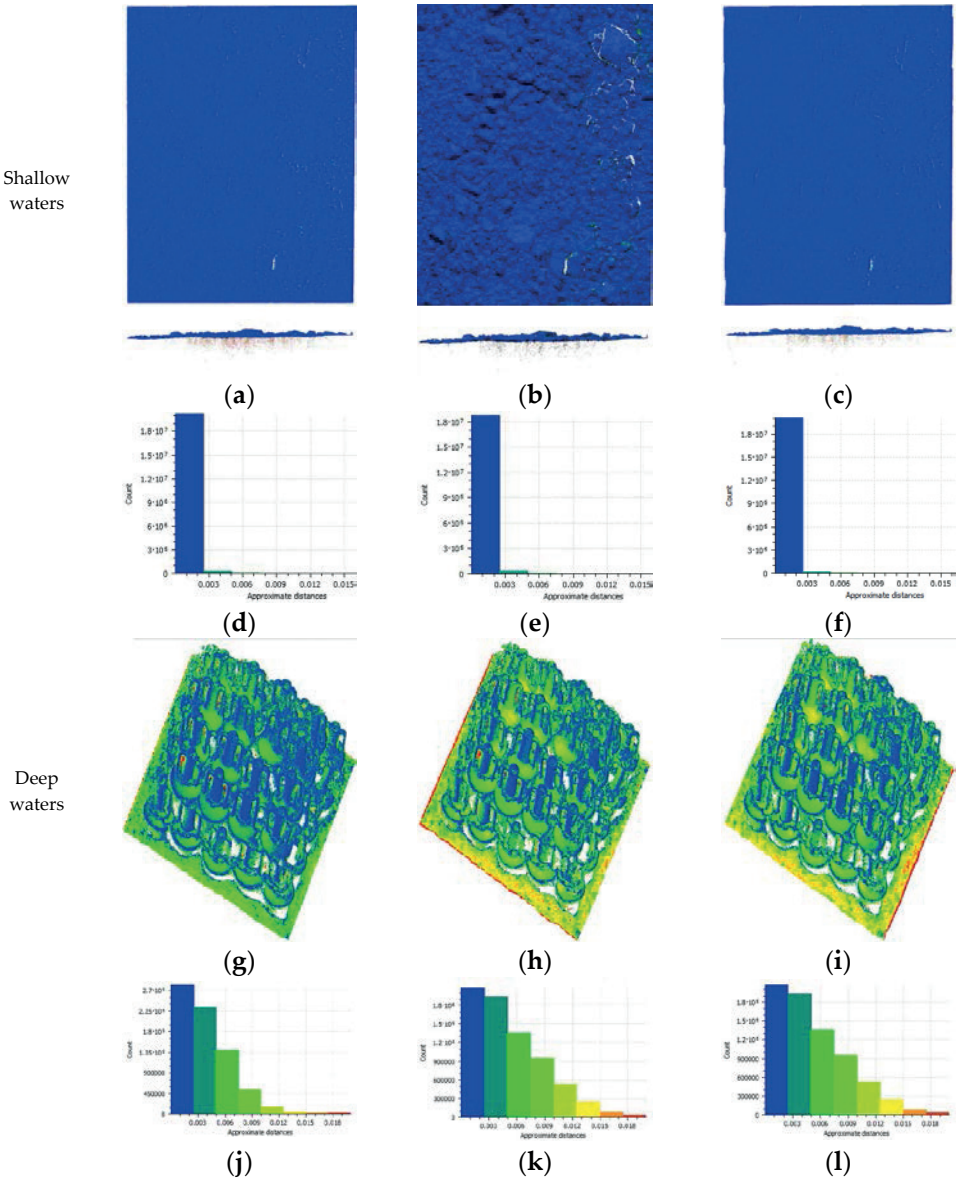

Figure 15. Three-dimensional point cloud (3Dpc) comparisons in Cloud Compare: The results of the comparison of the 3Dpc of the shallow waters test site (**a–c**) and histograms of deviations from the 3Dpc of the original images for shallow waters: CLAHE-shallow (**d**), Bianco et al. (2015) (**e**), Photoshop (**f**) and for deep waters the results of the comparisons (**g–i**) and histograms of deviations from the 3Dpc of the original images CLAHE-deep (**j**), Bianco et al. (2015) (**k**), Photoshop (**l**).

Table 2. Differences between 3Dpcs in Cloud Compare. 3Dpc from the original photos is considered as reference.

Compared 3D Point Clouds		Point Cloud Differences (m)			Percentage of Points That Deviate		
		Max	Mean	Sigma	0–0.0025m	0.0025–0.01m	0.01–0.02m
Shallow waters	Original- CLAHE based Algorithm	0.02	1.01-05	0.00005	91%	9%	
	Original- Lab based algorithm	0.02	0.65-05	0.00040			
	Original.-Photoshop	0.02	0.40-05	0.00030			
Deep waters	Original- CLAHE based Algorithm	0.02	0.001	0.00400	34%	49%	17%
	Original- Lab based algorithm	0.02	0.002	0.00500	26%	72.5%	1.5%
	Original.-Photoshop	0.02	0.002	0.00600	23%	69.8%	7.2%

As it is observed, the results of the comparison of the 3D point clouds of the deep waters dataset have larger percentages of errors in relation with the 3D point clouds of the shallow water dataset. This is because of the different complexity of the objects in the dataset, as well as the impact of the increased depth to the original colours. Additionally, it is noted that for the shallow depth dataset, the 3D point cloud comparisons resulted in almost the same percentages, and this is due to the small depth and mainly due to the non-complex captured environment. These are also confirmed by Table 2, showing that the mean and the sigma of the differences between 3D point clouds in Cloud Compare are smaller for the shallow test site. Regarding the differences in the GSD of the two datasets, they are considered of minor importnace since both of the GSDs are sub-millimetered (Table 1). Moreover, even if the 3D point cloud of the CLAHE based corrected images presents the largest percentage of points that differ less than 0.0025 m from the point cloud resulting from the original images, the 3D point cloud of the images resulting from the correction of Bianco et al., (2015) has most of its points between 0.0025 and 0.01 m while it presents the smallest percentage of deviations larger than 0.01 m for deep waters dataset. However, the 3D point clouds resulting from all the correction algorithms do not present any important deviation from the 3D point cloud of the original imagery. Most of these insignificant differences are resulting mainly due to the noise that is introduced by the alteration of the image radiometry, a fact that may mislead the image matching algorithm. Following the figures of Table 2, one may assume that the colour correction technique with more effect to the 3Dpc with respect to the original, is the CLAHE. If total percentage of difference below 0.01m is taken into consideration, the remaining two techniques, have less effect to the 3Dpc. Nevertheless, this effect may be either a diminishment or an improvement.

As already mentioned, the underwater environment affects the underwater image radiometry, even in shallow waters. Results show that the number of automatically generated 3Dpc points is increased for each image enhancment method, without providing useful extra information, where, in some cases, adding

noise to the object. The specific image enhancement techniques on shallow and deep depth underwater imagery do not seem to affect the 3D reconstruction. Colour correction before automated photogrammetric procedure does not seem to have any important impact on the final orthoimage, and, as such, the stage of using the specific image enhancement processes is subjective. However, this result it seems is strongly dependeny on the colour correction method used. Results showed that this is valid for the 5/6 of the tests and comparisons perfomed and presented in this article, while for the rest 1/6; the comparison between Figures 9d and 10d (Adobe photoshop results for shallow water dataset) does not apply since the direct colour correction of the orthoimage using Adobe Photoshop has results.

4. Concluding Remarks

When it comes to underwater orthoimage production applications, the underwater image pre-processing seems unnecessary, since simply the colour enhancement and correction of the produced orthoimages is sufficient and time efficient. In more detatil, the tested enhancement and correction methods do not seem to significantly improve 3D reconstruction effectiveness in Agisoft's Photoscan software and for the selected types of test sites and depths using the specific cameras. Point cloud comparisons in Cloud Compare software showed minor differences in the relevant accuracy, when the noise is ignored. In addition, orthoimages subtraction did not suggest any important differences. The image enhancement methods that are mentioned above improve the image visual quality and make them more appealing for the human eye. However, they do not improve feature detection and matching on the SfM process and overall 3D reconstruction in the specific SfM - MVS software in non turbid water, while in high turbidity water seems to be effective enough (Mahiddine et al., 2012). This result can be explained by the fact that the colour correction and enhancement methods used exploit the already stored information of the image. This also points out the robustness of the keypoint detection algorithm that is used. Additonally, these results might suggest that Agisoft Photoscan software, while using three-channel RGB images, might create and use a different channel (i.e. luminance channel) for applying SfM-MVS processing, and, as such, the colour correction and enhancment methods do not affect directly the SfM-MVS results.

Future work should include more tests by using more test sites of different depths and complexity, and by exploiting more colour correction and enhancment algorithms and SfM-MVS software, as well as all-purpose photogrammetric tools, like GRAPHOS (González-Aguilera et al, 2016), which integrates different algorithms and methodologies for automated image orientation and dense 3D reconstruction. Finally, recent research results indicate that the colour correction of the textures of a 3D model is a fast and reliable way to improve the visual quality of an underwater 3D model without enchanching the source image dataset.

Acknowledgments: The authors would like to acknowledge the Department of Fisheries and Marine Research of Cyprus, for the creation and permission to use the artificial amphorae reef, in this paper. Additionally, the authors would like to acknowledge the 3D Research s.r.l. member Antonio Lagudi for providing the implementation of the algorithm Bianco et al. 2015. The contribution of Dimitrios Skarlatos and Panagiotis Agrafiotis was partially supported by iMARECULTURE project (Advanced VR, iMmersive Serious Games and Augmented REality as Tools to Raise Awareness and Access to European Underwater CULTURal heritagE, Digital Heritage) that has received funding from the European Union's Horizon 2020 research and innovation programme under grant agreement No 727153.

References

1. Adobe Photoshop CS5 (Software), 2010. Available online: https://www.adobe.com/products/photoshop.html.
2. Agisoft LLC. Agisoft PhotoScan User Manual: Professional Edition; 2017.
3. Agrafiotis, P.; Drakonakis, G.I.; Georgopoulos, A.; Skarlatos, D. The effect of underwater imagery radiometry on 3d reconstruction and orthoimagery. *Int. Arch. Photogramm. Remote Sens. Spat. Inf. Sci.* **2017**, *XLII-2/W3*, 25–31, doi:10.5194/isprs-archives-XLII-2-W3-25-2017.
4. Bianco, G.; Muzzupappa, M.; Bruno, F.; Garcia, R.; Neumann, L. A new color correction method for underwater imaging. *Int. Arch. Photogramm. Remote Sens. Spat. Inf. Sci.* **2015**, *XL-5/W5*, 25–32, doi:10.5194/isprsarchives-XL-5-W5-25-2015.
5. Bruno, F.; Lagudi, A.; Ritacco, G.; Agrafiotis, P.; Skarlatos, D.; Čejka, J.; Kouřil, P.; Liarokapis, F.; Philpin-Briscoe, O.; Poullis, C.; et al. Development and integration of digital technologies addressed to raise awareness and access to European underwater cultural heritage. An overview of the H2020 i-MARECULTURE project. In Proceedings of OCEANS 2017, Aberdeen, UK, 19–22 June 2017; pp. 1–10, doi:10.1109/OCEANSE.2017.8084984.
6. CloudCompare (Version 2.8.1) [GPL Software], 2016. Available online: http://www.cloudcompare.org/.
7. Demesticha, S. The 4th-Century-BC Mazotos Shipwreck, Cyprus: A preliminary report. *Int. J. Naut. Archaeol.* **2011**, *40*, 9–59.
8. Drap, P. Underwater photogrammetry for archaeology. In *Special Applications of Photogrammetry*; InTech Open: Rijeka, Croatia, 2012.
9. Ghani, A.S.A.; Isa, N.A.M. Underwater image quality enhancement through composition of dual-intensity images and rayleigh-stretching. *SpringerPlus* **2014**, *3*, 757.
10. González-Aguilera, D.; López-Fernández, L.; Rodriguez-Gonzalvez, P.; Guerrero, D.; Hernandez-Lopez, D.; Remondino, F.; Menna, F.; Nocerino, E.; Toschi, I.; Ballabeni, A.; et al. Development of an all-purpose free photogrammetric tool. *Int. Arch. Photogramm. Remote Sens. Spat. Inf. Sci.* **2016**, *XLI-B6*, 31–38, doi:10.5194/isprs-archives-XLI-B6-31-2016.
11. Henderson, J.; Pizarro, O.; Johnson-Roberson, M.; Mahon, I. Mapping submerged archaeological sites using stereo-vision photogrammetry. *Int. J. Naut. Archaeol.* **2013**, *42*, 243–256.

12. Hitam, M.S.; Awalludin, E.A.; Yussof, W.N.J.H.W.; Bachok, Z. Mixture contrast limited adaptive histogram equalization for underwater image enhancement. In Proceedings of the 2013 International Conference on Computer Applications Technology (ICCAT), Sousse, Tunisia, 20–22 January 2013; pp. 1–5.
13. Hou, W.; Weidemann, A.D.; Gray, D.J.; Fournier, G.R. Imagery-derived modulation transfer function and its applications for underwater imaging. *Proc. SPIE* **2007**, *6696*, doi: 10.1117/12.734953.
14. Iqbal, K.; Abdul Salam, R.; Osman, M.; Talib, A.Z. Underwater image enhancement using an integrated colour model. *IAENG Int. J. Comput. Sci.* **2007**, *32*, 239–244.
15. Johnson-Roberson, M.; Bryson, M.; Friedman, A.; Pizarro, O.; Troni, G.; Ozog, P.; Henderson, J.C. High-resolution underwater robotic vision-based mapping and three-dimensional reconstruction for archaeology. *J. Field Robot.* **2017**, 34, 625–643.
16. Kumar Rai, R.; Gour, P.; Singh, B. Underwater image segmentation using clahe enhancement and thresholding. *Int. J. Emerg. Technol. Adv. Eng.* **2012**, 2, 118–123.
17. Mahiddine, A.; Seinturier, J.; Boi, D.P.J.-M.; Drap, P.; Merad, D.; Long, L. Underwater image preprocessing for automated photogrammetry in high turbidity water: An application on the arles-rhone xiii roman wreck in the Rhodano river, France. In Proceedings of the 2012 18th International Conference on Virtual Systems and Multimedia (VSMM), Milan, Italy, 2–5 September 2012; pp. 189–194.
18. Singh, B.; Mishra, R.S.; Gour, P. Analysis of contrast enhancement techniques for underwater image. *Int. J. Comput. Technol. Electron. Eng.* **2011**, *1*, 190–194.
19. Treibitz, T.; Schechner, Y.Y. Active polarization descattering. *IEEE Trans. Pattern Anal. Mach. Intell.* **2009**, *31*, 385–399.
20. Von Lukas, U.F. Underwater visual computing: The grand challenge just around the corner. *IEEE Comput. Graph. Appl.* **2016**, *36*, 10–15.
21. Yussof, W.; Hitam, M.S.; Awalludin, E.A.; Bachok, Z. Performing contrast limited adaptive histogram equalization technique on combined color models for underwater image enhancement. *Int. J. Interact. Digit. Media* **2013**, *1*, 1–6.
22. Zuiderveld, K. Contrast Limited Adaptive Histogram Equalization. In *Graphics GEMS IV*; Academic Press Professional, Inc.: San Diego, CA, USA, 1994; pp. 474–485.

Agrafiotis, P.; Drakonakis, G.I.; Skarlatos, D. Underwater Image Enhancement before Three-Dimensional (3D) Reconstruction and Orthoimage Production Steps: Is It Worth? In *Latest Developments in Reality-Based 3D Surveying and Modelling*; Remondino, F., Georgopoulos, A., González-Aguilera, D., Agrafiotis, P., Eds.; MDPI: Basel, Switzerland, 2018; pp. 239–256.